blood®
Plenary Paper

THROMBOSIS AND HEMOSTASIS

Antiphospholipid antibodies induce thrombosis by PP2A activation via apoER2-Dab2-SHC1 complex formation in endothelium

Anastasia Sacharidou,[1] Ken L. Chambliss,[1] Victoria Ulrich,[1] Jane E. Salmon,[2] Yu-Min Shen,[3] Joachim Herz,[4] David Y. Hui,[5] Lance S. Terada,[3] Philip W. Shaul,[1,*] and Chieko Mineo[1,*]

[1]Center for Pulmonary and Vascular Biology, Department of Pediatrics, University of Texas Southwestern Medical Center, Dallas, TX; [2]Department of Medicine, Hospital for Special Surgery, Weill Cornell Medical College, New York, NY; [3]Department of Internal Medicine and [4]Molecular Genetics, University of Texas Southwestern Medical Center, Dallas, TX; and [5]Department of Pathology, College of Medicine, University of Cincinnati, Cincinnati, OH

KEY POINTS

- **The activation of PP2A in endothelium underlies thrombus formation induced by aPL in mice.**
- **Endothelial apoER2 serves as a scaffold for aPL-induced assembly of a Dab2 and SHC1-containing complex that assembles and activates PP2A.**

In the antiphospholipid syndrome (APS), antiphospholipid antibody (aPL) recognition of β2 glycoprotein I promotes thrombosis, and preclinical studies indicate that this is due to endothelial nitric oxide synthase (eNOS) antagonism via apolipoprotein E receptor 2 (apoER2)-dependent processes. How apoER2 molecularly links these events is unknown. Here, we show that, in endothelial cells, the apoER2 cytoplasmic tail serves as a scaffold for aPL-induced assembly and activation of the heterotrimeric protein phosphatase 2A (PP2A). Disabled-2 (Dab2) recruitment to the apoER2 NPXY motif promotes the activating L309 methylation of the PP2A catalytic subunit by leucine methyl transferase-1. Concurrently, Src homology domain-containing transforming protein 1 (SHC1) recruits the PP2A scaffolding subunit to the proline-rich apoER2 C terminus along with 2 distinct regulatory PP2A subunits that mediate inhibitory dephosphorylation of Akt and eNOS. In mice, the coupling of these processes in endothelium is demonstrated to underlie aPL-invoked thrombosis. By elucidating these intricacies in the pathogenesis of APS-related thrombosis, numerous potential new therapeutic targets have been identified. (*Blood*. 2018;131(19):2097-2110)

Introduction

In individuals suffering from the antiphospholipid syndrome (APS), circulating anti-phospholipid antibodies (aPLs)[1-3] greatly increase the risk for thrombosis and for other cardiovascular morbidities and mortality.[4,5] In a recent study of 1000 APS patients followed over 10 years, 31% of subjects suffered thrombotic events despite anticoagulant therapy, and transient ischemic attacks, strokes, deep vein thrombosis, and pulmonary embolism were common.[6] In addition, aPL positivity is found in 14% of stroke, 11% of myocardial infarction, and 10% of deep vein thrombosis patients.[7] Regrettably, currently available therapies for APS are limited to long-term anticoagulation, which is expensive, inconvenient, and fraught with complications including hemorrhage and osteoporosis.[8,9] As such, there is an unmet need for more efficacious, mechanism-directed therapies for the thrombotic diathesis that characterizes this disorder.

In APS, high titers of aPL against the protein β2 glycoprotein I (β2GPI) are particularly closely associated with thrombotic events.[1,10] APL interaction with β2GPI engages transmembrane receptors including apolipoprotein E receptor 2 (apoER2; LRP8) to modify intracellular signaling and alter aPL target cell behavior. We and others have shown that the global deletion of apoER2 in mice affords protection from aPL-induced thrombosis, and we further revealed that a critical distal step is the antagonism of endothelial nitric oxide (NO) synthase (eNOS) and resulting deficiency of the antithrombotic-signaling molecule NO.[11,12] However, how aPL recognition of β2GPI is molecularly linked via apoER2 to eNOS antagonism and in what aPL target cell this occurs in vivo to mediate thrombosis are unknown.

Seeking to better understand the mechanistic underpinnings of APS-related thrombosis, experiments were designed to test the hypothesis that cytoplasmic domains of apoER2 serve to couple aPL recognition of β2GPI to alterations in eNOS enzymatic activity. Noting that endothelial cells and platelets both express apoER2 and eNOS,[11-16] we also determined the relative role of endothelial cell apoER2 in disease pathogenesis in vivo in mice. Additional genetic and pharmacologic measures were useded in mice to translate the mechanistic findings in cultured endothelial cells to APS-related thrombosis in vivo.

Methods

Animal models

In vivo studies were performed in wild-type (WT) C57BL/6 mice, littermate WT mice (apoER2-WT), knock-in mice expressing

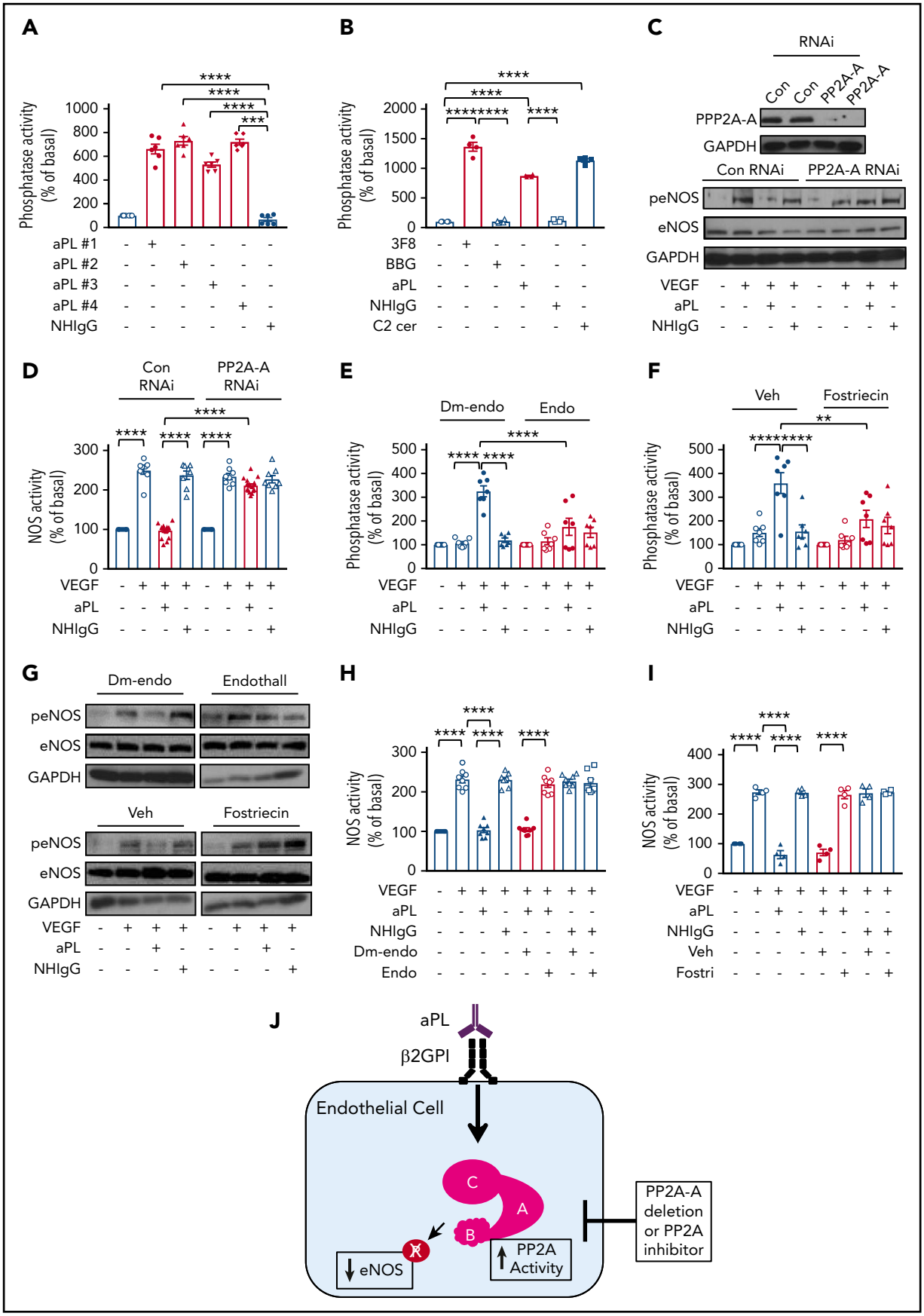

Figure 1.

full-length WT apoER2 (apoER2-FL), mutant apoER2 with NFDNPVY substituted by EIGNPVY (apoER2-EIG), or apoER2 lacking exon 19 (apoER2-Δ19) on identical 129SvEv × C57BL/6J backgrounds.[17,18] Male mice were studied at 4 to 5 weeks of age. ApoER2$^{fl/fl}$ mice were created by insertion of loxP sites flanking exons 1 and 2 (supplemental Figure 1A, available on the *Blood* Web site). A detailed description is provided in supplemental Materials and methods. The apoER2$^{fl/fl}$ mice were backcrossed to C57BL/6 for >8 generations. ApoER2$^{fl/fl}$ mice were crossed with mice expressing Cre-recombinase under the regulation of the vascular endothelial cadherin promoter (VECadCre, from M. Luisa Iruela-Arispe, UCLA, Los Angeles, CA)[19] to generate mice lacking apoER2 selectively in endothelium (apoER2ΔEC). All animal experiments were approved by the institutional animal care and utilization committees at the University of Texas Southwestern Medical Center.

Antibody preparation

Normal human immunoglobulin G (NHIgG) and aPLs were isolated from healthy individuals and APS patients as previously described.[11,20-22] The relevant clinical and laboratory features of the APS patients are provided in supplemental Materials and methods. Written informed consent was provided before study participation. All protocols were approved by the institutional review boards of the Hospital for Special Surgery and the University of Texas Southwestern Medical Center. Mouse monoclonal antibody directed against β2GPI (designated 3F8) and its isotype-matched control (designated BBG) were generated as previously described.[11,23,24]

Dab1 and Dab2 expression

Human umbilical vein endothelial cell (HUVEC) and human aortic endothelial cell (HAEC) expression of Disabled-1 (Dab1) and Dab2 was assessed by reverse transcription–polymerase chain reaction (see details in supplemental Materials and methods).

Adenoviral apoER2 constructs

Human WT apoER2 complementary DNA was used for site-directed mutagenesis according to the manufacturer's protocol (Agilent Technologies). The apoER2-EIG construct was generated by Vivogen Biotechnology, Inc. All of the mutations were verified by sequencing. Primers used for mutagenesis to produce apoER2-NPVA and apoER2-Δ59 are provided in supplemental Materials and methods.

Cell culture, siRNA, and adenoviral transfection

HAECs and HUVECs were purchased by Lonza, cultured in EGM-2+Bullet kit media (Lonza), and used within 3 to 5 passages. In siRNA experiments, HAECs were transfected with the small interfering RNAs (siRNAs) shown in supplemental Materials and methods (ThermoFisher) using siPORT Amine transfection reagent as previously described.[25] Control siRNA was purchased from GE Dharmacon (ON-TARGETplus Non-targeting Control siRNA). Briefly, HAECs were first transfected with siRNA targeting endogenous apoER2, and subsequently the cells were transfected with adenoviral particles (10^{10} particles per milliliter) encoding apoER2 constructs. Experiments were performed 18 hours postadenoviral transfection.

eNOS activation assay

Activation of eNOS was assessed in HAECs by measuring the conversion of [^{14}C] L-arginine to [^{14}C] L-citrulline as described previously.[11] Briefly, cells were preincubated with NHIgG or aPL (100 μg/mL for 90 minutes) and eNOS activity was determined over 30 minutes in the continued presence of NHIgG or aPL, and in the absence (basal) or presence of vascular endothelial growth factor (VEGF; 100 ng/mL). In select experiments, HAECs were incubated with siRNA or adenoviral particles before eNOS activation was assessed. In separate sets of experiments, HAECs were treated for 4 hours with the protein phosphatase 2A (PP2A) inhibitor endothall (10 μM) or its control 1-4-Dimethylendothall (10 μM), or with Fostriecin (10 μM) vs its vehicle control (methanol) prior to the assessment of eNOS activity. All findings were replicated in 3 or more independent experiments.

Phosphatase assay

PP2A phosphatase activity was evaluated using PP2A immunoprecipitation (IP) and a phosphatase assay kit (EMD 17-313). Cells were incubated for 90 minutes with NHIgG or aPL (100 μg/mL), in the absence (basal) or presence of VEGF (100 ng/mL), or with C2-ceramide (30 μM) serving as positive control. Lysates were generated and IP was performed with anti-PP2A catalytic subunit (PP2A-C) antibody immobilized on agarose beads for 2 hours. Immunoprecipitated PP2A was incubated with phosphorylated peptide substrate for 20 minutes at 30°C. Malachite green reagent was then used to quantify free phosphate abundance.

IP and immunoblot analysis

HAECs were lysed, and IP and immunoblotting were performed, as described in detail in supplemental Materials and methods.

Mass spectrometry

Following protein separation by sodium dodecyl sulfate polyacrylamide gel electrophoresis, gel samples were digested overnight with trypsin (Pierce) followed by reduction and alkylation with dithiothreitol and iodoacetamide (Sigma-Aldrich). After solid-phase extraction cleanup with Oasis HLB plates (Waters), the samples were analyzed by liquid chromatography–tandem mass spectrometry (LC-MS/MS) using an Orbitrap Fusion Lumos mass spectrometer (Thermo Electron) coupled to an

Figure 1. APL activation of PP2A underlies eNOS antagonism in endothelial cells. (A) HAECs were exposed to aPLs from 4 different APS patients or NHIgG (100 μg/mL) for 90 minutes, and PP2A activity was measured in cell lysates; N = 6. (B) PP2A activity was determined in HAECs exposed to anti-β2GPI monoclonal antibody (3F8, 10 μg/mL), its isotype-matched control (BBG, 10 μg/mL), NHIgG, or aPLs. Additional HAECs were incubated with C2-ceramide (30 μM) for 4 hours to provide a positive control; N = 4. (C) HAECs were transfected with control RNAi or RNAi targeting the PP2A A subunit (PP2A-A), and 24 hours later treated with aPLs or NHIgG followed by vehicle (phosphate-buffered saline [PBS]) or VEGF (100 ng/mL) for 30 minutes. Cell lysates were immunoblotted for phosphorylated-eNOS S1177 (peNOS), total eNOS, and glyceraldehyde-3-phosphate dehydrogenase (GAPDH). Findings shown were confirmed in 3 independent experiments. (D) In HAECs transfected and treated as in panel C, VEGF (100 ng/mL) activation of NOS activity was assessed in intact cells by measuring ^{14}C-arginine conversion to ^{14}C-citrulline; N = 6. (E-G) HAECs were incubated with the inactive analog 1,4-dimethyl-endothall (Dm-endo, 10 μM) vs endothall (Endo, 10μM) for 4 hours (E,G), or with vehicle (Veh, methanol) vs Fostriecin (Fostri, 10 μM) for 4 hours (F-G), and with aPLs vs NHIgG, and vehicle vs VEGF. In cell lysates, PP2A activity was quantified (E-F, n = 7) and immunoblotting for peNOS, total eNOS, and GAPDH was performed (G, findings were confirmed in 3 independent experiments). (H-I) In studies paralleling those in panels E-G, VEGF stimulation of NOS activity was evaluated in intact cells; N = 6. In graphs, values are mean ± SEM, ****$P < .0001$, ***$P < .001$, and **$P < .01$. (J) Summary of findings in the figure.

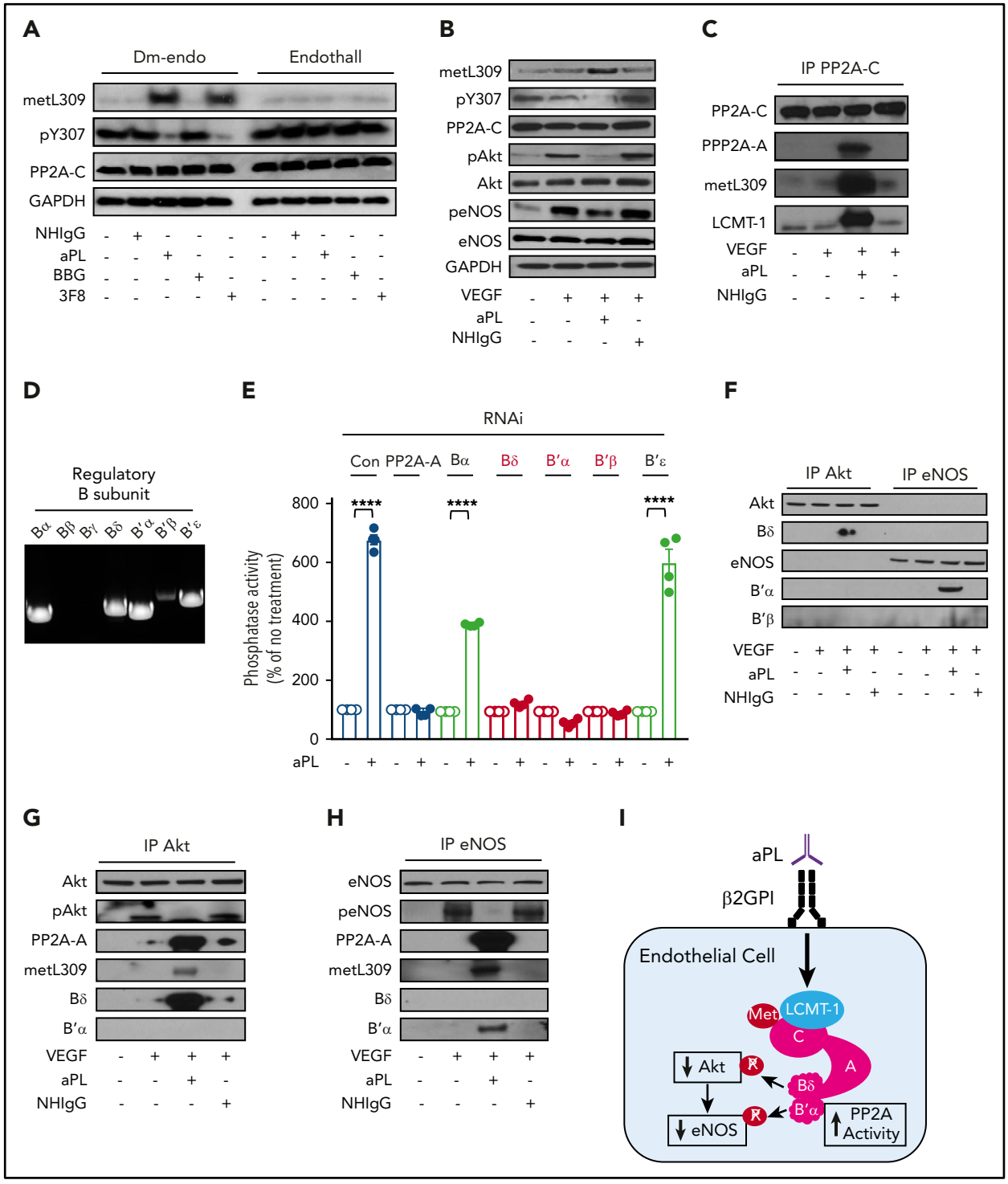

Figure 2. APL promote PP2A-C L309 methylation and Y307 dephosphorylation, PP2A subunit assembly, and PP2A-B Bδ and B′α recruitment to Akt and eNOS as selective phosphoprotein substrates in endothelial cells. (A) HAECs were treated with NHIgG, aPLs (100 μg/mL), BBG or 3F8 (10 μg/mL) in the presence of the inactive analog Dm-endo or endothall (10 μM) for 90 minutes, and with vehicle (PBS) or VEGF (100 ng/mL) for 30 minutes, cell lysates were prepared, and immunoblot analysis was performed detecting methylated PP2A-C L309 (metL309), phosphorylated PP2A-C Y307 (pY307), total PP2A-C and GAPDH. (B) HAECs were treated with NHIgG or aPLs (100 μg/mL) for 90 minutes, and with vehicle (PBS) or VEGF (100 ng/mL) for 30 minutes, and immunoblot analysis was performed detecting methylated PP2A-C L309 (metL309), phosphorylated PP2A-C Y307 (pY307), total PP2A-C, and GAPDH. Immunoblotting was also performed for Akt phosphorylation at S473 (p-Akt), total Akt (Akt), phosphorylated eNOS at S1177 (peNOS), and total eNOS (eNOS). (C) In parallel studies, PP2A-C was immunoprecipitated, and the co-IP of PP2A-A and LCMT-1 was evaluated along with PP2A-C metL309. (D) Reverse transcription–polymerase chain reaction was performed to detect transcripts for PP2A-B subunits Bα, Bβ, Bγ, Bδ, B′α, B′β, and B′ε in HAECs. (E) HAECs were transfected with control RNAi or RNAi targeting PP2A-Aα, or PP2A-B subunit Bα, Bδ, B′α, B′β, or B′ε; 24 hours later, the cells were treated with aPLs or NHIgG (100 μg/mL) for 90 minutes, and PP2A activity was quantified in cell lysates; N = 4. Values are mean ± SEM, ****$P < .0001$. (F-H) HAECs were treated as in panel B, Akt or eNOS was immunoprecipitated, and the co-IP of PP2A-A, PP2A-C metL309, Bδ, B′α, and B′β was evaluated along with immunoblotting for pAkt and peNOS. Findings in all immunoblots were confirmed in 3 independent experiments. (I) Summary of the findings in the figure.

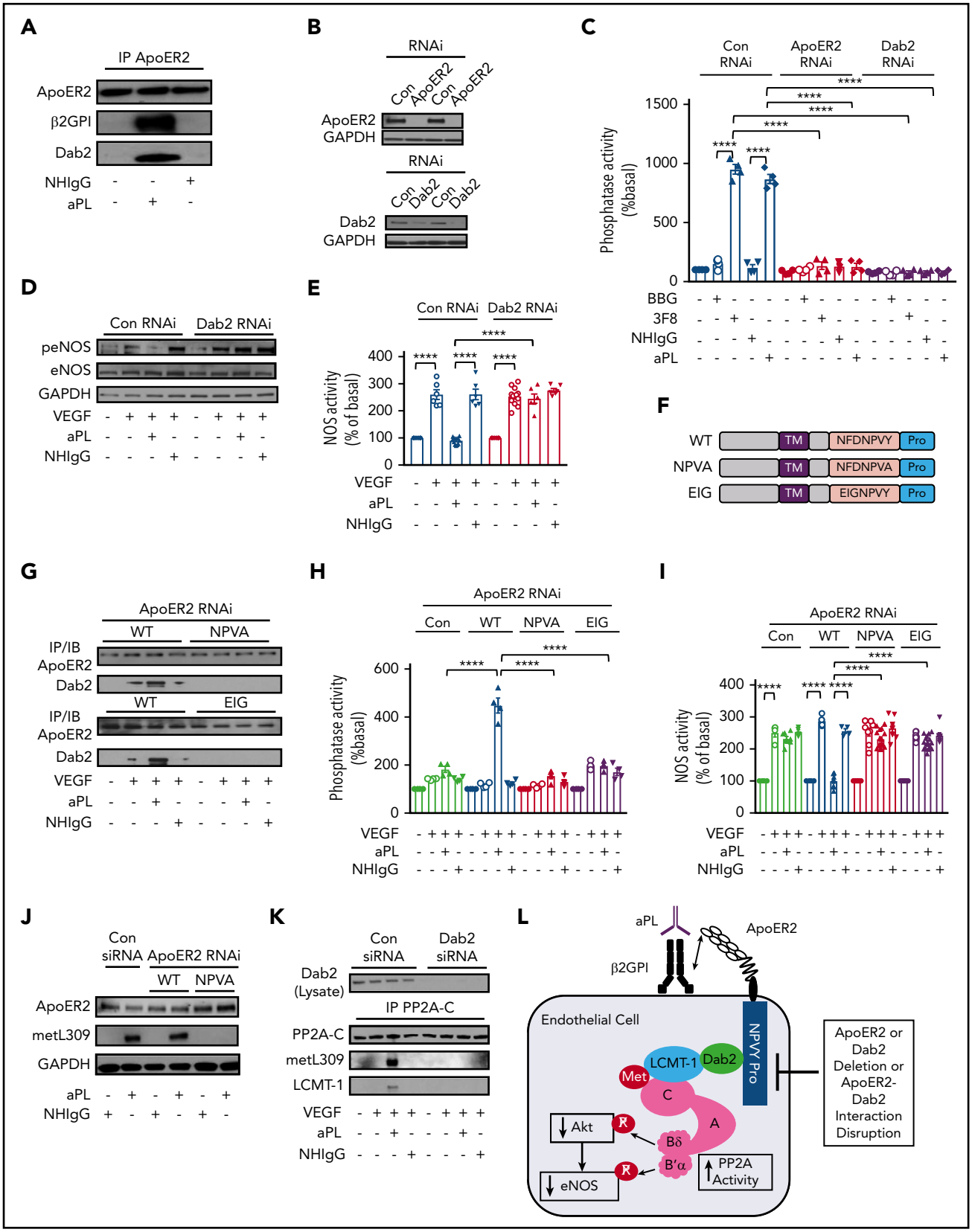

Figure 3. Dab2 recruitment to apoER2 via the NPXY motif is required for aPL induction of PP2A activity by LCMT-1 interaction with PP2A-C in endothelial cells, and for resulting eNOS antagonism. (A) HAECs were treated with vehicle, NHIgG, or aPLs (100 μg/mL) for 90 minutes, cell lysates were prepared, apoER2 was immunoprecipitated, and the co-IP of β2GPI and Dab2 was evaluated by immunoblotting. (B-C) HAECs were transfected with control RNAi (Con RNAi) or RNAi targeting apoER2 or Dab2; 24 hours later they were treated with BBG or 3F8 (10 μg/mL), or NHIgG or aPL (100 μg/mL) for 90 minutes, and lysates were prepared to detect apoER2 and Dab2 by immunoblotting (B) or to quantify PP2A activity (C, n = 4). (D-E) HAECs were transfected with control RNAi or RNAi targeting Dab2; 24 hours later, they were treated with NHIgG or aPLs, and vehicle or

Ultimate 3000 RSLC-Nano liquid chromatography system (Dionex). Raw MS data files were converted to a peak list format and analyzed using the central proteomics facilities pipeline, version 2.0.3.[26,27] Peptide identification was performed using the X! Tandem and Open MS Search Algorithm (OMSSA) search engines against a human protein database from Uniprot.[28-30]

Intravital microscopy

Thrombus formation was assessed as previously described.[11,20] Briefly, 24 hours following injection with either NHIgG or aPL (100 μg, IP), alone or in conjunction with endothall (10 μmol/kg body weight) or 1,4-dimethyl-endothall,[31] mice (males, 4-6 weeks old) were IV injected with fluorescence-labeled anti-mouse GPIbβ antibody. The mesenteric microcirculation was exteriorized and thrombus formation was induced by 10% ferric chloride solution placed on Whatman filter paper for 45 seconds Thrombus formation in 80- to 100-μm arterioles was documented by capturing images every 1 second for 25 minutes with a QuantEm 512S camera attached to a Nikon Eclipse Ti microscope with NIS Element image-capturing software.

Statistical analysis

All data are expressed as mean ± standard error of the mean (SEM). Statistical analyses were performed using GraphPad Prism (version 7.01). One-way analysis of variance and Tukey post hoc testing were used to assess differences among groups. In cell culture studies, the findings reported were confirmed in at least 3 independent experiments. *P* values <.05 were considered significant.

Results

APL activation of PP2A is required for eNOS antagonism

The activation of eNOS by multiple agonists including VEGF requires eNOS S1177 phosphorylation,[32,33] and we previously showed that aPLs suppress VEGF-induced eNOS S1177 phosphorylation and enzyme activation.[11] Because in various paradigms the serine/threonine PP2A dephosphorylates eNOS S1177,[34-36] we determined whether aPLs stimulate PP2A activity in HAECs. In contrast to polyclonal NHIgG from healthy individuals, polyclonal aPLs from 4 different APS patients stimulated PP2A activity by fivefold to sevenfold (Figure 1A). Using C2 ceramide as a positive control,[37-39] potent activation of PP2A was also observed in HAECs treated with the monoclonal anti-β2GPI antibody (3F8), which mimics aPL action,[11,20] whereas its subtype-matched control IgG (BBG) had no effect (Figure 1B). Active PP2A is a heterotrimeric holoenzyme composed of scaffolding (PP2A-A), regulatory (PP2A-B), and catalytic subunits (PP2A-C) designated A, B, and C, respectively.[40,41] Knockdown of PP2A-Aα (PR65α), a dominant form of PP2A-A in adult tissues,[42] by small RNA interference (RNAi) prevented aPL suppression of eNOS S1177 phosphorylation and enzyme activation induced by VEGF (Figure 1C-D; supplemental Figure 2A) (please note that in the overall schematic in Figure 6E, superscript numbers are provided to indicate the figure in which data are presented about a given molecule or structural feature of apoER2). The PP2A inhibitors endothall[31,43] and Fostriecin[44,45] effectively blunted PP2A activation in HAECs by aPLs (Figure 1E-F), and both agents prevented the inhibitory action of aPLs on eNOS S1177 phosphorylation and enzyme activation in response to VEGF (Figure 1G-I; supplemental Figure 2B). Thus, aPLs robustly stimulate PP2A activity in human endothelial cells, and the resulting PP2A activation is the basis for aPL antagonism of eNOS (Figure 1J).

The activity and substrate specificity of PP2A are regulated through posttranslational modifications of PP2A-C, which govern the binding of numerous possible PP2A-B subunits.[46,47] PP2A-B then targets specific phosphoprotein substrates to PP2A.[46,48,49] The most common posttranslational modifications of PP2A-C are Y307 phosphorylation and L309 methylation.[48,50-53] L309 methylation is mediated by leucine methyl-transferase 1 (LCMT-1), a 334-aa enzyme that shares little sequence similarity with other methyl-transferases.[54,55] LCMT-1 is responsible for carboxyl methylation of PP2A, and it enhances the affinity of PP2A-C for PP2A-B, resulting in modulation of the specificity of PP2A.[47,51,52,56,57] PP2A-C Y307 phosphorylation, which occurs when L309 is demethylated,[50,58] attenuates PP2A enzymatic activity. We found that whereas NHIgG has no effect, aPLs enhance PP2A-C L309 methylation and attenuate PP2A-C Y307 phosphorylation, and the PP2A inhibitor endothall negated both processes (Figure 2A). The aPL-related posttranslational modifications in PP2A-C occur coincidentally with diminished VEGF-induced phosphorylation of Akt at S473 and of eNOS at S1177 (Figure 2B). Furthermore, aPL treatment promotes the association of LCMT-1 with PP2A-C, which is highly methylated at L309 (Figure 2C), and the association of PP2A-C with PP2A-A.

The specific PP2A-B subunits that recruit Akt and eNOS for dephosphorylation were then identified. PP2A-B subunits are divided into 4 structurally distinct families designated B, B′, B′′, and B′′′.[53,59,60] Recognizing that B and B′ family members preferentially bind to modified PP2A-C at L309 and Y307 residues,[48,61-63] we determined which B or B′ family members are expressed in HAECs (Figure 2D). We found that HAECs do not express Bβ or Bγ, but they express Bα, Bδ, B′α, B′β, and B′ε. Using RNAi knockdown (supplemental Figure 3), we found that silencing of Bδ, B′α, or B′β inhibits aPL activation of PP2A to a similar extent as knockdown of PP2A-A (Figure 2E). In contrast, Bα and B′ε knockdown did not negate PP2A activation by aPL. We then evaluated whether aPLs promote the recruitment of Bδ, B′α, or B′β to Akt or eNOS (Figure 2F-H), and found that aPLs stimulate interaction between dephosphorylated Akt and L309-methylated PP2A-A and Bδ, and not the recruitment of B′α or B′β to Akt; aPL also induced

Figure 3 (continued) VEGF (100 ng/mL, 30 minutes), and immunoblotting was done to detect eNOS S1177 phosphorylation (peNOS), total eNOS, and GAPDH (D). With the same treatments, NOS activity was determined in intact cells (E, n = 6-12). (F-I) Endogenous apoER2 was silenced with RNAi, and using adenoviral constructs HA-tagged WT apoER2 (WT) or mutant forms of apoER2 harboring NFDNPVA (NPVA) or EIGNPVY (EIG) substitutions for NFDNPVA were reintroduced (F). Cells were treated 24 hours later with NHIgG or aPLs, and vehicle or VEGF; apoER2 was immunoprecipitated using anti-HA antibody, and Dab2 co-IP was evaluated by immunoblotting (G). In parallel studies, PP2A activity was quantified in cell lysates (H, n = 4), NOS activity was evaluated in intact cells (I, n = 8-16), and PP2A-C subunit methylation at L309 was assessed in cell lysates by immunoblotting (I). (J) Following control RNAi or RNAi silencing Dab2, 24 hours later, cells were treated with NHIgG or aPLs, and vehicle or VEGF; (K) PP2A-C was immunoprecipitated; and PP2A-C metL309 or total PP2A-C were detected by immunoblotting. The co-IP of LCMT-1 was also evaluated by immunoblotting. Values in graphs are mean ± SEM, ****$P < .0001$, and findings in all immunoblots were confirmed in 3 independent experiments. (L) Summary of the findings in the figure.

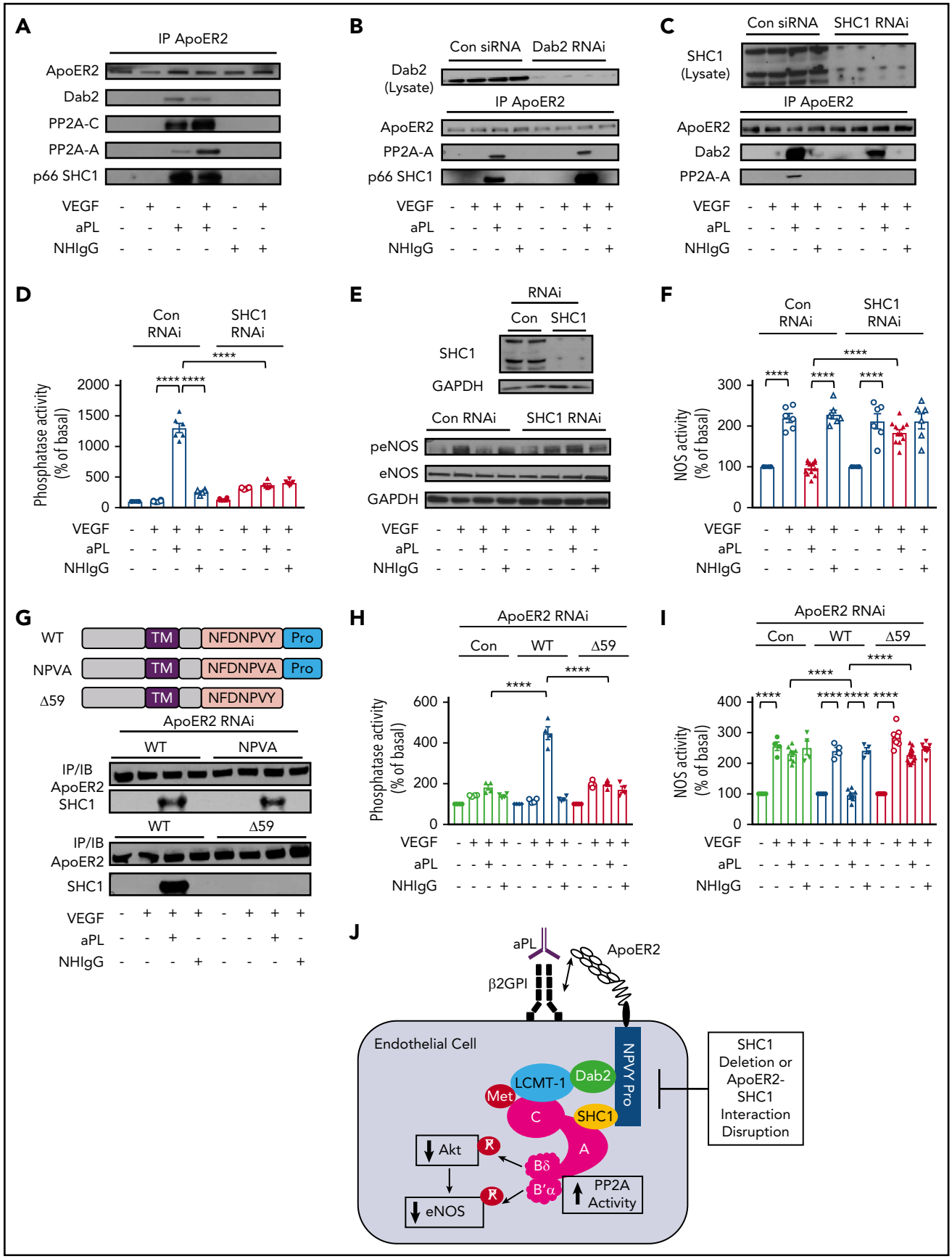

Figure 4. P66 SHC1 recruitment to apoER2 via the proline-rich C terminus of the receptor is required for PP2A-A recruitment in response to aPL, and the resulting activation of PP2A and eNOS antagonism in endothelial cells. (A) HAECs were treated with NHIgG or aPLs (100 μg/mL) for 90 minutes, and with vehicle or VEGF (100 ng/mL) for 30 minutes, apoER2 was immunoprecipitated, and the co-IP of Dab2, PP2A-C, PP2A-A, and p66 SHC1 was evaluated by immunoblotting. (B) HAECs were transfected with

interaction between dephosphorylated eNOS and L309-methylated PP2A-A and B′α, and not B′β or Bδ recruitment to eNOS. Thus, in human endothelial cells, aPLs stimulate PP2A association with LCMT-1 to increase PP2A-C L309 methylation, leading to the formation of the active heterotrimeric holoenzymes A-C-Bδ and A-C-B′α to cause inhibitory dephosphorylation of Akt and eNOS, respectively (Figure 2I).

Dab2 is required for aPL-induced PP2A activation

To identify apoER2-associated proteins required for aPL action in endothelial cells, HAECs were treated with NHIgG or aPL for 90 minutes, apoER2 was immunoprecipitated, and the immunoprecipitates were analyzed by LC-MS/MS (supplemental Table 1). As expected from our prior demonstration of aPL promotion of apoER2-β2GPI interaction,[11,20] sixfold more spectral counts were detected for β2GPI (also known as APOH) associated with apoER2 immunoprecipitated from HAECs treated with aPLs vs NHIgG. In addition, Dab2 was detected in apoER2 immunoprecipitates from cells treated with aPLs but not NHIgG. These results were confirmed by demonstrating the co-IP of β2GPI and Dab2 with apoER2 in aPL-treated HAECs (Figure 3A). Whereas Dab1 mediates apoER2 signaling in neurons, macrophages, and platelets,[64-67] we found that HAECs and HUVECs only express Dab2, and that mouse primary aortic endothelial cells express both Dab2 and Dab1 (supplemental Figure 4). To determine the relative requirement for Dab2 in aPL-induced PP2A activation, apoER2 or Dab2 was knocked down in HAECs (Figure 3B), and PP2A activation by the anti-β2GPI monoclonal antibody 3F8 or aPL was evaluated (Figure 3C). Loss of Dab2 or apoER2 prevented PP2A activation in response to 3F8 or aPL. In parallel, aPL suppression of VEGF-stimulated eNOS S1177 phosphorylation and eNOS enzymatic activity were dependent on both apoER2 (supplemental Figure 5) and Dab2 (Figure 3D-E; supplemental Figure 6).

Because Dab2 binds to members of the low-density lipoprotein (LDL) receptor family via their C-terminal NPXY sequence,[68] the requirement for Dab2-apoER2 interaction in aPL action in endothelial cells was tested by silencing endogenous apoER2 followed by adenovirus-driven reconstitution with C-terminally hemagglutinin (HA)-tagged WT apoER2 (NFDNPVY), or mutant receptor harboring NFDNPVA (NPVA) or EIGNPVY (EIG) sequence[17,69] (Figure 3F; supplemental Figure 7). In response to aPLs, there was a marked increase in Dab2 interaction with WT apoER2, but no association between Dab2 and either the NPVA or EIG mutant receptor (Figure 3G). We further demonstrated that whereas apoER2-WT expression restores aPL activation of PP2A and inhibition of eNOS stimulation by VEGF, the NPVA or EIG mutant forms of apoER2 fail to do so (Figure 3H-I). Moreover, we found that aPLs do not stimulate PP2A-C methylation at L309 in cells expressing the NPVA mutant (Figure 3J), and that Dab2 is required for aPL promotion of LCMT-1 recruitment to PP2A-C and resulting PP2A-C L309 methylation (Figure 3K). These collective findings indicate that aPLs induce Dab2 association with apoER2 via the apoER2 NFDNPXY domain, and that via its apoER2 interaction, Dab2 participates in PP2A activation by aPL by enabling LCMT-1 recruitment to PP2A-C to invoke L309 methylation (Figure 3L).

SHC1 is required for PP2A activation by aPL

Having determined that, via Dab2 recruitment to apoER2, aPLs promote the methylation of PP2A-C, we next determined whether PP2A-A is also recruited to the receptor. Consistent with LC-MS/MS revealing that fivefold more PP2A-A coimmunoprecipitates with apoER2 upon aPL treatment (supplemental Table 1), PP2A-A interaction with apoER2 was observed in aPL-exposed cells concurrent with the recruitment of Dab2 and PP2A-C (Figure 4A). Next, we determined whether Dab2 mediates PP2A-A recruitment to the apoER2 protein complex, and we found that PP2A-A interaction with the receptor is equally stimulated by aPL in cells expressing or lacking Dab2 (Figure 4B). This suggested involvement of a different adaptor protein, and we determined that p66 Src homology domain-containing transforming protein 1 (SHC1) is readily recruited to the apoER2 complex in the presence of aPL (Figure 4A). The aPL-induced recruitment of p66 SHC1 occurred independent of Dab2 (Figure 4B), and SHC1 was required for aPL promotion of PP2A-A interaction with apoER2 (Figure 4C). We also determined that SHC1 is required for PP2A activation by aPL (Figure 4D), and for aPL inhibition of VEGF stimulation of eNOS S1177 phosphorylation (Figure 4E; supplemental Figure 7) and eNOS enzymatic activity (Figure 4F).

To determine the basis for p66 SHC1 recruitment to apoER2 in response to aPLs, endogenous apoER2 was silenced and replaced with either WT apoER2, or mutant forms of the receptor disrupting the NPXY motif by substituting it with NPVA, or lacking the C-terminal 59-aa proline-rich domain of the receptor (Δ59; Figure 4G; supplemental Figure 8). p66 SHC1 recruitment to apoER2 in response to aPL was evident in endothelial cells expressing apoER2-WT, and it was conserved in cells expressing apoER2-NPVA (Figure 4G). In contrast, no interaction between apoER2 and SHC1 was observed in cells expressing apoER2-Δ59. Consistent with the requirement for the proline-rich C terminus of apoER2 in aPL-induced interaction of the receptor with p66 SHC1, in HAECs expressing apoER2-Δ59, aPL did not stimulate PP2A and there was a resulting failure of aPL to antagonize eNOS activation by VEGF (Figure 4H-I). These cumulative observations reveal that aPLs promote p66 SHC1 association with apoER2 primarily via the receptor's C-terminal proline-rich domain, and that this association is required for PP2A-A recruitment to apoER2, for PP2A enzyme activation, and for the inhibition of eNOS that occurs upon endothelial cell exposure to aPL (Figure 4J).

Figure 4 (continued) control RNAi or RNAi targeting Dab2; 24 hours later, they were treated with NHIgG or aPLs, and vehicle or VEGF, apoER2 was immunoprecipitated, and the co-IP of PP2A-A and p66 SHC1 was evaluated by immunoblotting. (C) Using a parallel approach, SHC1 was silenced; 24 hours later, cell treatments occurred and apoER2 was immunoprecipitated, and the co-IP of Dab2 and PP2A-A was evaluated. (D-F) Following SHC1 silencing and NHIgG vs aPLs and vehicle vs VEGF treatment, PP2A activity (D, n = 6-12) or eNOS S1177 phosphorylation (E) was evaluated in cell lysates, or NOS activity was assessed in intact cells (F, n = 6-12). (G) Endogenous apoER2 was silenced with RNAi, and using adenoviral constructs HA-tagged WT apoER2 (WT) or mutant forms of apoER2 harboring NFDNPVA (NPVA) substitution for NFDNPVA or lacking the proline-rich C terminus of the receptor (Δ59) were reintroduced. Cells were treated 24 hours later with NHIgG or aPLs, and vehicle or VEGF, apoER2 was immunoprecipitated using anti-HA antibody, and SHC1 co-IP was evaluated by immunoblotting. (H-I) In parallel studies, PP2A activity was quantified in cell lysates (H, n = 4) or NOS activity was evaluated in intact cells (I, n = 8-16). Values in graphs are mean ± SEM, $^{****}P < .0001$, and findings in all immunoblots were confirmed in 3 independent experiments. (J) Summary of the findings in the figure.

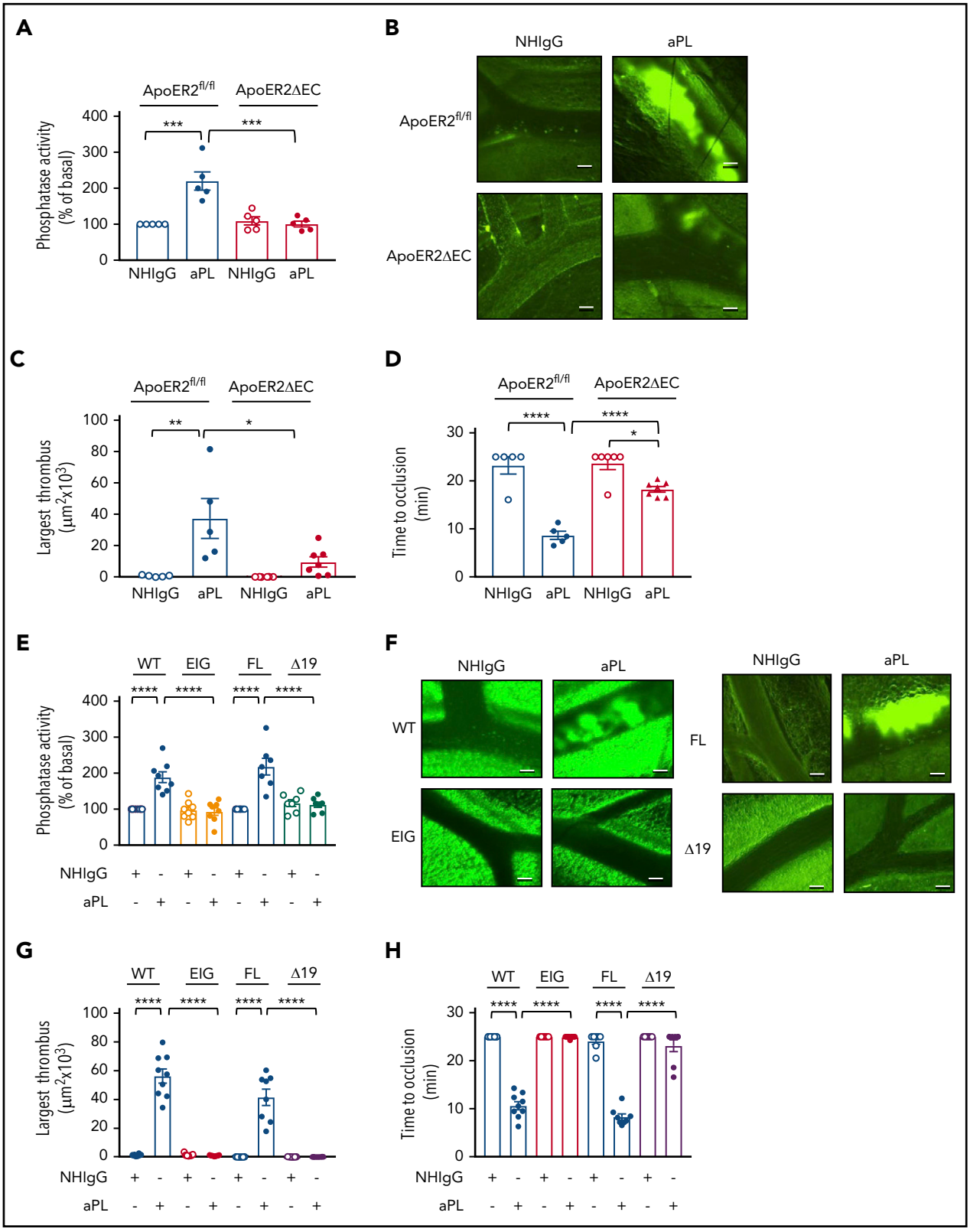

Figure 5. Mice lacking endothelial apoER2 or expressing mutant forms of apoER2 incapable of interaction with Dab2 or p66 SHC1 are protected from aPL-induced thrombosis. (A) Control ApoER2$^{fl/fl}$ or ApoER2ΔEC male mice (4-6 weeks old) were injected with NHIgG or aPL (100 μg, IP), and, 24 hours later, aortas were isolated and PP2A activity was quantified; N = 5. (B-D) Mice were treated as described in panel A, and thrombus formation following ferric chloride initiation was evaluated in the mesenteric microcirculation by intravital microscopy. Representative still images taken 9 minutes after ferric chloride application are shown in panel B. The size of the largest thrombi formed within 9 minutes of initiation (C) and time to total occlusion were evaluated (D). (C-D) N = 5-7. (E-H) The impact of aPL on thrombus formation was evaluated in control WT mice (WT) and control mice with full-length apoER2 (FL), and in mice expressing mutant forms of apoER2 harboring an EIGNPVY substitution for NFDNPVA (EIG) or lacking the proline-rich C terminus of the receptor (ApoER2Δ19) (N = 7-11). PP2A activity was measured in isolated aortas (E); representative images of thrombus formation 9 minutes after ferric

Endothelial apoER2 and apoER2 Dab2- and SHC1-binding domains are required for aPL-induced thrombosis

We next determined whether the apoER2 complex formation and related mechanisms revealed in cultured endothelial cells are operative in aPL-induced thrombosis in vivo in mice.[11,20] To test the requirement for endothelial apoER2, floxed apoER2 mice (apoER2$^{fl/fl}$) were generated (supplemental Figure 1A-B) and bred with mice expressing Cre recombinase under the regulation of the vascular endothelial cadherin promotor.[19,70] In the resulting mice lacking apoER2 selectively in endothelium (apoER2ΔEC), whereas apoER2 messenger RNA expression in bone marrow–derived myeloid cells was unaffected, transcript levels in endothelial cells were decreased 94% (supplemental Figure 1C-D). aPL or NHIgG was administered to apoER2$^{fl/fl}$ or apoER2ΔEC mice, and, 24 hours later, PP2A activity in aorta and thrombus formation in the mesenteric microcirculation was evaluated.[11,20] Whereas aorta PP2A activity was increased in apoER2$^{fl/fl}$ mice administered aPLs compared with those given NHIgG, aPLs did not activate PP2A in the aortas of apoER2ΔEC mice (Figure 5A). Thrombus formation, which was assessed by quantifying the size of the largest thrombus formed within 9 minutes after ferric chloride–induced initiation or the time to full occlusion, was predictably enhanced by aPL administration in control apoER2$^{fl/fl}$ mice (Figure 5B-D; supplemental Videos 1-4). In contrast, aPL-treated apoER2ΔEC mice had markedly smaller thrombi and longer time to vessel occlusion compared with apoER2$^{fl/fl}$ mice, with parameters equal to or approaching those observed with NHIgG.

The requirements for Dab2 and SHC1 interaction with apoER2 were evaluated using apoER2-EIG knock-in mice expressing apoER2 in which the NFDNPVY motif is altered to EIGNPVY (EIG), and apoER2Δ19 mice expressing apoER2 lacking the exon 19-encoded proline-rich C terminus.[17,18,71] Whereas control mice, either WT or those expressing full-length apoER2 (FL), displayed PP2A activation in the aorta in response to aPL (Figure 5E), apoER2-EIG and apoERΔ19 mice did not. In parallel, as indicated by either size of largest thrombus or time to occlusion, aPL-induced thrombosis was suppressed in apoER2-EIG and apoER2Δ19 mice (Figure 5F-H; supplemental Videos 5-12). These findings reveal that endothelial cells are a major target cell for aPL in APS-related thrombosis, and that the features of apoER2 required for receptor interaction with Dab2 and SHC1, which is necessary for heterotrimeric PP2A formation and activation in endothelium in response to aPLs, are indispensable for aPL provocation of thrombosis in vivo.

PP2A inhibition prevents aPL-induced thrombus formation

To evaluate the role of PP2A activation in aPL-induced thrombosis in vivo, WT mice were administered the PP2A inhibitor endothall or its inactive analog 1,4-dimethyl-endothall (Dm-Endo), and either NHIgG or aPL. Whereas aPL upregulated PP2A activity 4.5-fold compared with NHIgG in mice given Dm-Endo (Figure 6A), endothall prevented aPL activation of PP2A. In parallel, in endothall-treated mice markedly smaller thrombi formed in response to aPLs, and despite aPL exposure the time to vessel occlusion approached values for NHIgG (Figure 6B-D; supplemental Videos 13-16). Thus, pharmacologic antagonism of PP2A effectively prevents thrombus formation induced by aPLs in vivo.

Discussion

Individuals with APS are prone to episodes of thrombosis and they have increased risk for other cardiovascular morbidities and mortality.[1,3,6,7] In studies in cultured endothelial cells and mice, we previously demonstrated that the exaggerated thrombosis is driven by aPL recognition of β2GPI, which leads to eNOS antagonism and relative deficiency of the antithrombotic signaling molecule NO, through processes involving the LDL receptor family member apoER2.[11,20] In the present work, we have delineated the molecular links between aPL binding to β2GPI and eNOS inhibition. We have discovered that in response to aPL recognition of β2GPI, which causes β2GPI dimerization and interaction with apoER2,[11] an apoER2-Dab2-SHC1 complex forms in endothelial cells to assemble and activate the heterotrimeric protein phosphatase PP2A (Figure 6E). Dab2 recruitment to the apoER2 NPXY motif enables activating L309 methylation of the PP2A-C by recruited LCMT-1, and concurrently SHC1 recruits the PP2A-A to the proline-rich apoER2 C terminus. Completing the PP2A heterotrimer formation prompted by aPLs, 2 distinct regulatory PP2A subunits (PP2A-B), Bδ and B′α, provide substrate specificity and recruit Akt and eNOS, respectively, to cause their inhibitory dephosphorylation and consequent NO deficiency, which promotes thrombosis. By elucidating these intricacies in the pathogenesis of APS-related thrombosis, numerous potential new therapeutic targets have been identified.

Complementing the dissection of how PP2A heterotrimer formation and enzyme activation occur in response to aPLs, we reveal that PP2A inhibition in vivo dramatically attenuates thrombus formation in mice administered aPL. Other conditions in which PP2A activity contributes to disease pathogenesis include obesity-induced hypertension, type 2 diabetes, and inflammatory lung disorders such as chronic obstructive pulmonary disease and asthma.[37,72] The present studies are the first to signify that the inhibition of PP2A is a potential therapeutic option in APS-related thrombosis. Because PP2A is involved in a variety of pivotal cellular processes,[46,48,53] it is recognized that broad-based, long-term PP2A antagonism may have adverse effects. However, having identified Bδ and B′α in endothelium as the specific PP2A-B subunits by which aPL activation of PP2A designates endothelial Akt and eNOS as target phosphoproteins, the use of small cell-permeable molecules to disrupt their discrete interactions with other PP2A subunits or their phosphoprotein prey may represent viable therapeutic options.[73,74]

In the present studies, Dab2 and SHC1 have been identified as the critical adaptor proteins linking heterotrimeric PP2A to apoER2 in aPL-exposed endothelial cells. We reveal that Dab2 is

Figure 5 (continued) chloride application are shown (F); and the size of the largest thrombi formed within 9 minutes (G) and time to total occlusion were evaluated (H). (B, F) The images were captured by a Nikon Eclipse Ti microscope and its camera system (Quantem 512SC, Plan Fluor, 10×, 0.3 aperture) at room temperature with fluorescein isothiocyanate as fluorochrome. NIS Elements software was used to capture and process the images. Scale bars, 50 μm. Values are mean ± SEM, ****$P < .0001$, ***$P < .001$, **$P < .01$, *$P < .05$.

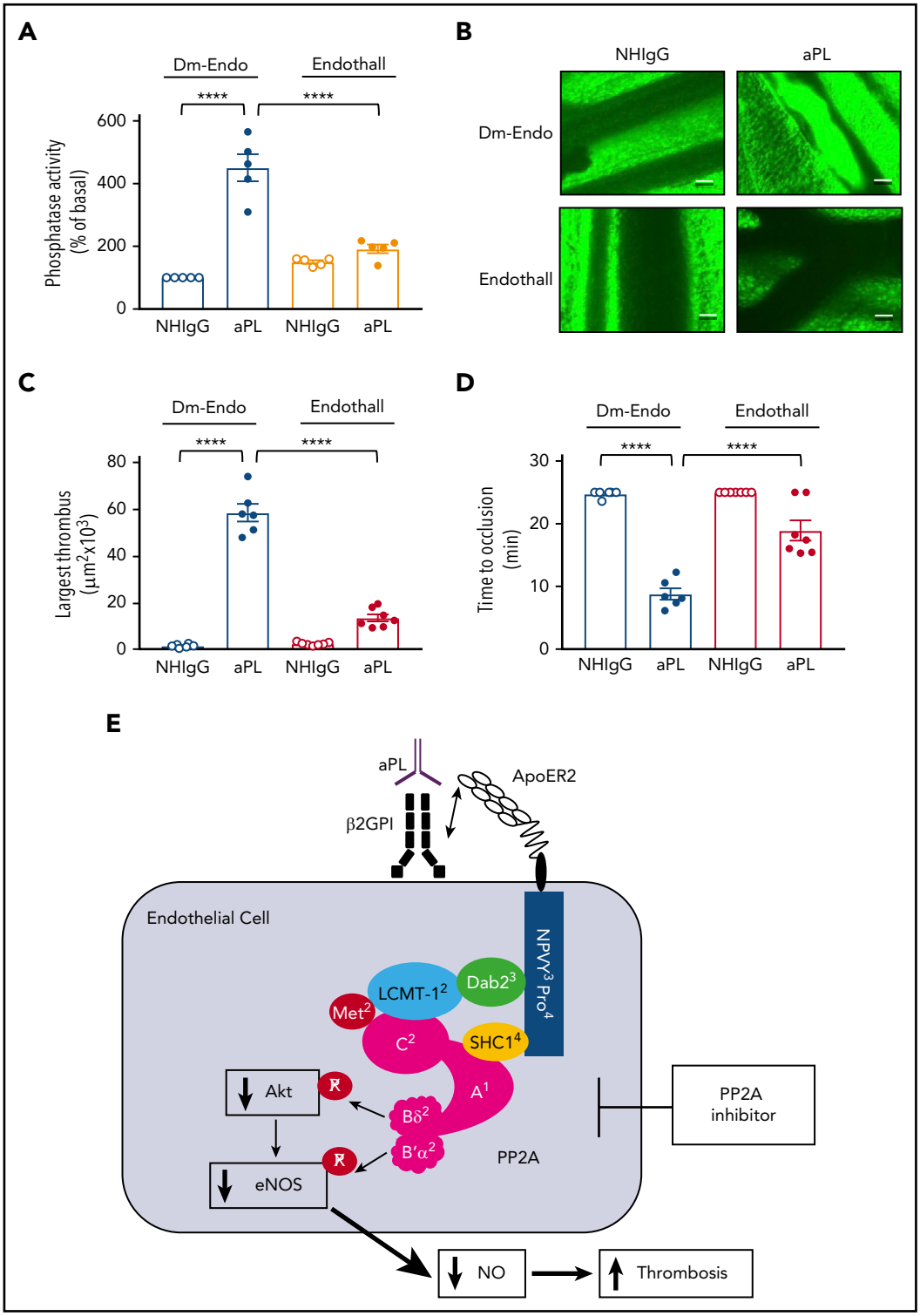

Figure 6. PP2A inhibition prevents vascular PP2A activation and thrombus formation induced by aPL in mice. (A) Male C57BL/6 mice (4-6 weeks old) were injected with NHIgG or aPL (100 μg IP) in conjunction with the PP2A inhibitor endothall (10 μmol/kg body weight) or the control compound 1,4-dimethyl-endothall (Dm-Endo), and, 24 hours later, aortas were isolated and PP2A activity was quantified; N = 5. (B-D) Mice were treated as described in panel A, and thrombus formation following ferric chloride initiation was evaluated in the mesenteric microcirculation by intravital microscopy. (B) Representative still images taken 9 minutes after ferric chloride application are shown. The images were captured with a Nikon Eclipse Ti microscope and its camera system (Quantem 512SC, Plan Fluor, 10×, 0.3 aperture) at room temperature with fluorescein isothiocyanate as fluorochrome. NIS Elements software was used to capture and process the images. Scale bars, 50 μm. (C-D) The size of the largest thrombi formed within 9 minutes of initiation (C) and time to total occlusion were evaluated (D). In panels C and D, N = 5-6. Values are mean ± SEM, ****$P < .0001$. Scale bars, 50 μm. (E) Molecular basis of APS. PP2A subunits A, Bδ, B′α, and C are shown in magenta, and posttranslational modifications are shown in red. The superscript numbers indicate the figure in which data are presented about the molecule or structural feature of apoER2, and its participation in the molecular basis of APS. In response to aPL recognition of cell surface β2GPI, resulting β2GPI dimerization and interaction with apoER2, an apoER2-Dab2-SHC1 complex forms in endothelial cells to assemble and activate the heterotrimeric protein phosphatase PP2A. Dab2 recruitment to the apoER2 NPXY motif enables activating L309 methylation of PP2A-C by recruited LCMT-1. Concurrently, SHC1 recruits the PP2A-A to the proline-rich apoER2 C terminus along with 2 distinct regulatory PP2A subunits (PP2A-B), Bδ and B′α, to cause inhibitory dephosphorylation of Akt and eNOS, respectively. The resulting NO deficiency promotes thrombosis.

required for aPL-induced recruitment of LCMT-1 to PP2A-C to invoke PP2A-C L309 methylation. X-ray crystal structure studies of the LCMT-1–PP2A-C complex suggest that a conformational change in PP2A-C is required for binding of the methyltransferase.[75] We speculate that the dynamic interactions between apoER2, Dab2, and PP2A-C, which are prompted by aPLs, result in a change in PP2A-C 3-dimensional structure that facilitates its interaction with LCMT-1 and the methylation of PP2A-C L309. Regarding SHC1, in endothelial cells, we recently identified an interaction of SHC1 with p115-RhoGEF that is required for RhoA activation via SHC1 and the sensing of adhesion status by anchorage-dependent endothelial cells.[76,77] SHC1 has been associated with the modulation of eNOS activity previously, with its downregulation enhancing Akt and eNOS activation and the abundance of bioavailable NO.[78,79] However, the present work is the first to demonstrate SHC1 participation in a PP2A-related protein complex and PP2A activation. aPL-induced interactions between apoER2 and Dab2 and SHC1, as well as the observed Dab2 and SHC1 interactions with PP2A subunits, may offer additional opportunities for mechanism-directed interventions to combat thrombosis in APS.

Prior elucidation of the processes underlying APS-related thrombosis has benefited greatly from experiments performed ex vivo in platelets and endothelial cells, evaluating changes in their function by aPL.[11,80,81] Such work identified the 2 cell types as potential aPL targets in disease pathogenesis. However, determining whether endothelial cells or platelets are critical aPL target cells in which disease-related processes are initiated in vivo has been elusive. We leveraged the obligate participation of apoER2[11] and cell type–specific gene deletion in mice to directly address this issue. We found that aPL-treated mice lacking apoER2 selectively in endothelium have dramatically attenuated thrombosis, with parameters equal to or approaching those observed with control treatment with NHIgG. As such, the endothelium is a major aPL target cell in APS-related thrombosis, and new, mechanism-based therapies against the thrombosis can be directed at the endothelium. An endothelial focus for preventive and therapeutic interventions against APS moving forward is potentially advantageous because strategies for endothelial cell phenotype manipulation in vivo continue to emerge, such as the use of helper-dependent adenovirus to provide stable transgene expression in the endothelium.[82,83] Nonviral technology using polymeric nanoparticles for endothelial siRNA delivery is also gaining momentum,[84,85] with endothelial-avid nanoparticles enabling multigene silencing already becoming feasible.[86] Now having greater understanding of the molecular underpinnings of the disease, and the cell type in which the processes likely primarily take place, there is hope that the development and application of mechanism-based therapies against APS-related thrombosis has become more feasible.

Acknowledgments

This work was supported by National Institutes of Health National Heart, Lung, and Blood Institute grants T32HL098040 (A.S.), R01HL109604 (C.M.), R01HL118001 (D.Y.H. and P.W.S.), and R37HL63762 (J.H.), National Institute on Aging grant RF1AG053391 (J.H.), National Institute of Neurological Disorders and Stroke grant R01NS093382 (J.H.), and National Cancer Institute grant R01CA208620 (L.S.T.); the Hartwell Foundation (P.W.S.); the Crystal Charity Ball Center for Pediatric Critical Care Research and the Children's Medical Center Foundation (P.W.S.); and the Cancer Prevention and Research Institute of Texas RP160307 (L.S.T.).

Authorship

Contribution: A.S. designed and performed the experiments, analyzed the data, and wrote the manuscript; K.L.C., J.H., V.U., and D.Y.H. generated the genetically modified apoER2 mouse strains and performed their initial characterization; J.E.S. and Y.-M.S. recruited the individuals who provided the human IgG-based reagents; L.S.T. provided the reagents required for SHC1-related studies and aided in experimental design; P.W.S. and C.M. designed the experiments, analyzed the data, and wrote the manuscript; and all authors provided feedback on the manuscript.

Conflict-of-interest disclosure: The authors declare no competing financial interests.

Correspondence: Philip W. Shaul, Center for Pulmonary and Vascular Biology, Department of Pediatrics, University of Texas Southwestern Medical Center, 5323 Harry Hines Blvd, Dallas, TX 75390; e-mail: philip.shaul@utsouthwestern.edu; and Chieko Mineo, Center for Pulmonary and Vascular Biology, Department of Pediatrics, University of Texas Southwestern Medical Center, 5323 Harry Hines Blvd, Dallas, TX 75390; e-mail: chieko.mineo@utsouthwestern.edu.

Footnotes

Submitted 3 November 2017; accepted 23 February 2018. Prepublished online as *Blood* First Edition paper, 2 March 2018; DOI 10.1182/blood-2017-11-814681.

*P.W.S. and C.M. contributed equally to this study.

The online version of this article contains a data supplement.

There is a *Blood* Commentary on this article in this issue.

The publication costs of this article were defrayed in part by page charge payment. Therefore, and solely to indicate this fact, this article is hereby marked "advertisement" in accordance with 18 USC section 1734.

REFERENCES

1. Giannakopoulos B, Krilis SA. The pathogenesis of the antiphospholipid syndrome. *N Engl J Med*. 2013;368(11):1033-1044.

2. Miyakis S, Lockshin MD, Atsumi T, et al. International consensus statement on an update of the classification criteria for definite antiphospholipid syndrome (APS). *J Thromb Haemost*. 2006;4(2):295-306.

3. Ruiz-Irastorza G, Crowther M, Branch W, Khamashta MA. Antiphospholipid syndrome. *Lancet*. 2010;376(9751):1498-1509.

4. Amaya-Amaya J, Rojas-Villarraga A, Anaya JM. Cardiovascular disease in the antiphospholipid syndrome. *Lupus*. 2014;23(12):1288-1291.

5. Ambrosino P, Lupoli R, Tortora A, et al. Cardiovascular risk markers in patients with primary aldosteronism: a systematic review and meta-analysis of literature studies. *Int J Cardiol*. 2016;208:46-55.

6. Cervera R, Serrano R, Pons-Estel GJ, et al; Euro-Phospholipid Project Group (European Forum on Antiphospholipid Antibodies). Morbidity and mortality in the antiphospholipid syndrome during a 10-year period: a multicentre prospective study of 1000 patients. *Ann Rheum Dis*. 2015;74(6):1011-1018.

7. Chighizola CB, Andreoli L, de Jesus GR, Banzato A, Pons-Estel GJ, Erkan D; APS ACTION. The association between antiphospholipid antibodies and pregnancy morbidity, stroke, myocardial infarction, and

deep vein thrombosis: a critical review of the literature. *Lupus*. 2015;24(9):980-984.

8. de Jesus GR, Agmon-Levin N, Andrade CA, et al. 14th International Congress on Antiphospholipid Antibodies Task Force report on obstetric antiphospholipid syndrome. *Autoimmun Rev*. 2014;13(8):795-813.

9. Ruiz-Irastorza G, Cuadrado MJ, Ruiz-Arruza I, et al. Evidence-based recommendations for the prevention and long-term management of thrombosis in antiphospholipid antibody-positive patients: report of a task force at the 13th International Congress on antiphospholipid antibodies. *Lupus*. 2011;20(2):206-218.

10. de Groot PG, Urbanus RT. The significance of autoantibodies against β2-glycoprotein I. *Blood*. 2012;120(2):266-274.

11. Ramesh S, Morrell CN, Tarango C, et al. Antiphospholipid antibodies promote leukocyte-endothelial cell adhesion and thrombosis in mice by antagonizing eNOS via β2GPI and apoER2. *J Clin Invest*. 2011;121(1):120-131.

12. Romay-Penabad Z, Aguilar-Valenzuela R, Urbanus RT, et al. Apolipoprotein E receptor 2 is involved in the thrombotic complications in a murine model of the antiphospholipid syndrome. *Blood*. 2011;117(4):1408-1414.

13. Cozzi MR, Guglielmini G, Battiston M, et al. Visualization of nitric oxide production by individual platelets during adhesion in flowing blood. *Blood*. 2015;125(4):697-705.

14. Freedman JE, Loscalzo J, Barnard MR, Alpert C, Keaney JF, Michelson AD. Nitric oxide released from activated platelets inhibits platelet recruitment. *J Clin Invest*. 1997;100(2):350-356.

15. Pennings MT, Derksen RH, Urbanus RT, Tekelenburg WL, Hemrika W, de Groot PG. Platelets express three different splice variants of ApoER2 that are all involved in signaling. *J Thromb Haemost*. 2007;5(7):1538-1544.

16. Riddell DR, Vinogradov DV, Stannard AK, Chadwick N, Owen JS. Identification and characterization of LRP8 (apoER2) in human blood platelets. *J Lipid Res*. 1999;40(10):1925-1930.

17. Beffert U, Durudas A, Weeber EJ, et al. Functional dissection of Reelin signaling by site-directed disruption of Disabled-1 adaptor binding to apolipoprotein E receptor 2: distinct roles in development and synaptic plasticity. *J Neurosci*. 2006;26(7):2041-2052.

18. Masiulis I, Quill TA, Burk RF, Herz J. Differential functions of the Apoer2 intracellular domain in selenium uptake and cell signaling. *Biol Chem*. 2009;390(1):67-73.

19. Alva JA, Zovein AC, Monvoisin A, et al. VE-Cadherin-Cre-recombinase transgenic mouse: a tool for lineage analysis and gene deletion in endothelial cells. *Dev Dyn*. 2006;235(3):759-767.

20. Mineo C, Lanier L, Jung E, et al. Identification of a monoclonal antibody that attenuates antiphospholipid syndrome-related pregnancy complications and thrombosis. *PLoS One*. 2016;11(7):e0158757.

21. Ulrich V, Konaniah ES, Lee WR, et al. Antiphospholipid antibodies attenuate endothelial repair and promote neointima formation in mice. *J Am Heart Assoc*. 2014;3(5):e001369.

22. Ulrich V, Gelber SE, Vukelic M, et al. ApoE receptor 2 mediation of trophoblast dysfunction and pregnancy complications induced by antiphospholipid antibodies in mice. *Arthritis Rheumatol*. 2016;68(3):730-739.

23. He J, Luster TA, Thorpe PE. Radiation-enhanced vascular targeting of human lung cancers in mice with a monoclonal antibody that binds anionic phospholipids. *Clin Cancer Res*. 2007;13(17):5211-5218.

24. Ran S, He J, Huang X, Soares M, Scothorn D, Thorpe PE. Antitumor effects of a monoclonal antibody that binds anionic phospholipids on the surface of tumor blood vessels in mice. *Clin Cancer Res*. 2005;11(4):1551-1562.

25. Sacharidou A, Koh W, Stratman AN, Mayo AM, Fisher KE, Davis GE. Endothelial lumen signaling complexes control 3D matrix-specific tubulogenesis through interdependent Cdc42- and MT1-MMP-mediated events. *Blood*. 2010;115(25):5259-5269.

26. Trudgian DC, Mirzaei H. Cloud CPFP: a shotgun proteomics data analysis pipeline using cloud and high performance computing. *J Proteome Res*. 2012;11(12):6282-6290.

27. Trudgian DC, Thomas B, McGowan SJ, Kessler BM, Salek M, Acuto O. CPFP: a central proteomics facilities pipeline. *Bioinformatics*. 2010;26(8):1131-1132.

28. Craig R, Beavis RC. TANDEM: matching proteins with tandem mass spectra. *Bioinformatics*. 2004;20(9):1466-1467.

29. Geer LY, Markey SP, Kowalak JA, et al. Open mass spectrometry search algorithm. *J Proteome Res*. 2004;3(5):958-964.

30. Elias JE, Gygi SP. Target-decoy search strategy for increased confidence in large-scale protein identifications by mass spectrometry. *Nat Methods*. 2007;4(3):207-214.

31. Erdödi F, Tóth B, Hirano K, Hirano M, Hartshorne DJ, Gergely P. Endothall thioanhydride inhibits protein phosphatases-1 and -2A in vivo. *Am J Physiol*. 1995;269(5 Pt 1):C1176-C1184.

32. Fulton D, Gratton JP, McCabe TJ, et al. Regulation of endothelium-derived nitric oxide production by the protein kinase Akt [published correction appears in *Nature*. 1999;400(6746):792]. *Nature*. 1999;399(6736):597-601.

33. Shaul PW. Regulation of endothelial nitric oxide synthase: location, location, location. *Annu Rev Physiol*. 2002;64(1):749-774.

34. Michell BJ, Chen Zp, Tiganis T, et al. Coordinated control of endothelial nitric-oxide synthase phosphorylation by protein kinase C and the cAMP-dependent protein kinase. *J Biol Chem*. 2001;276(21):17625-17628.

35. Greif DM, Kou R, Michel T. Site-specific dephosphorylation of endothelial nitric oxide synthase by protein phosphatase 2A: evidence for crosstalk between phosphorylation sites. *Biochemistry*. 2002;41(52):15845-15853.

36. Mineo C, Gormley AK, Yuhanna IS, et al. FcgammaRIIB mediates C-reactive protein inhibition of endothelial NO synthase. *Circ Res*. 2005;97(11):1124-1131.

37. Bharath LP, Ruan T, Li Y, et al. Ceramide-initiated protein phosphatase 2A activation contributes to arterial dysfunction in vivo. *Diabetes*. 2015;64(11):3914-3926.

38. Mehra VC, Jackson E, Zhang XM, et al. Ceramide-activated phosphatase mediates fatty acid-induced endothelial VEGF resistance and impaired angiogenesis. *Am J Pathol*. 2014;184(5):1562-1576.

39. Zhang QJ, Holland WL, Wilson L, et al. Ceramide mediates vascular dysfunction in diet-induced obesity by PP2A-mediated dephosphorylation of the eNOS-Akt complex. *Diabetes*. 2012;61(7):1848-1859.

40. Mumby MC, Walter G. Protein serine/threonine phosphatases: structure, regulation, and functions in cell growth. *Physiol Rev*. 1993;73(4):673-699.

41. Oliver CJ, Shenolikar S. Physiologic importance of protein phosphatase inhibitors. *Front Biosci*. 1998;3(4):D961-D972.

42. Kiely M, Kiely PA. PP2A: the wolf in sheep's clothing? *Cancers (Basel)*. 2015;7(2):648-669.

43. Li YM, Mackintosh C, Casida JE. Protein phosphatase 2A and its [3H]cantharidin/[3H] endothall thioanhydride binding site. Inhibitor specificity of cantharidin and ATP analogues. *Biochem Pharmacol*. 1993;46(8):1435-1443.

44. Buck SB, Hardouin C, Ichikawa S, et al. Fundamental role of the fostriecin unsaturated lactone and implications for selective protein phosphatase inhibition. *J Am Chem Soc*. 2003;125(51):15694-15695.

45. Walsh AH, Cheng A, Honkanen RE. Fostriecin, an antitumor antibiotic with inhibitory activity against serine/threonine protein phosphatases types 1 (PP1) and 2A (PP2A), is highly selective for PP2A. *FEBS Lett*. 1997;416(3):230-234.

46. Sontag E. Protein phosphatase 2A: the Trojan horse of cellular signaling. *Cell Signal*. 2001;13(1):7-16.

47. Xu Y, Xing Y, Chen Y, et al. Structure of the protein phosphatase 2A holoenzyme. *Cell*. 2006;127(6):1239-1251.

48. Janssens V, Longin S, Goris J. PP2A holoenzyme assembly: in cauda venenum (the sting is in the tail). *Trends Biochem Sci*. 2008;33(3):113-121.

49. Lambrecht C, Haesen D, Sents W, Ivanova E, Janssens V. Structure, regulation, and pharmacological modulation of PP2A phosphatases. *Methods Mol Biol*. 2013;1053:283-305.

50. Chen J, Parsons S, Brautigan DL. Tyrosine phosphorylation of protein phosphatase 2A in response to growth stimulation and v-src transformation of fibroblasts. *J Biol Chem*. 1994;269(11):7957-7962.

51. Xing Y, Li Z, Chen Y, Stock JB, Jeffrey PD, Shi Y. Structural mechanism of demethylation and inactivation of protein phosphatase 2A. *Cell*. 2008;133(1):154-163.

52. Tolstykh T, Lee J, Vafai S, Stock JB. Carboxyl methylation regulates phosphoprotein phosphatase 2A by controlling the association of regulatory B subunits. *EMBO J*. 2000;19(21):5682-5691.

53. Janssens V, Goris J. Protein phosphatase 2A: a highly regulated family of serine/threonine phosphatases implicated in cell growth and signalling. *Biochem J*. 2001;353(Pt 3):417-439.

54. De Baere I, Derua R, Janssens V, et al. Purification of porcine brain protein phosphatase 2A leucine carboxyl methyltransferase and cloning of the human homologue. *Biochemistry*. 1999;38(50):16539-16547.

55. Leulliot N, Quevillon-Cheruel S, Sorel I, et al. Structure of protein phosphatase methyltransferase 1 (PPM1), a leucine carboxyl methyltransferase involved in the regulation of protein phosphatase 2A activity. *J Biol Chem*. 2004;279(9):8351-8358.

56. Ogris E, Gibson DM, Pallas DC. Protein phosphatase 2A subunit assembly: the catalytic subunit carboxy terminus is important for binding cellular B subunit but not polyomavirus middle tumor antigen. *Oncogene*. 1997;15(8):911-917.

57. Shi Y. Serine/threonine phosphatases: mechanism through structure. *Cell*. 2009;139(3):468-484.

58. Chen J, Martin BL, Brautigan DL. Regulation of protein serine-threonine phosphatase type-2A by tyrosine phosphorylation. *Science*. 1992;257(5074):1261-1264.

59. Lechward K, Awotunde OS, Swiatek W, Muszyńska G. Protein phosphatase 2A: variety of forms and diversity of functions. *Acta Biochim Pol*. 2001;48(4):921-933.

60. Virshup DM. Protein phosphatase 2A: a panoply of enzymes. *Curr Opin Cell Biol*. 2000;12(2):180-185.

61. Longin S, Zwaenepoel K, Louis JV, Dilworth S, Goris J, Janssens V. Selection of protein phosphatase 2A regulatory subunits is mediated by the C terminus of the catalytic subunit. *J Biol Chem*. 2007;282(37):26971-26980.

62. Nunbhakdi-Craig V, Schuechner S, Sontag JM, et al. Expression of protein phosphatase 2A mutants and silencing of the regulatory B alpha subunit induce a selective loss of acetylated and detyrosinated microtubules. *J Neurochem*. 2007;101(4):959-971.

63. Park JH, Sung HY, Lee JY, Kim HJ, Ahn JH, Jo I. B56α subunit of protein phosphatase 2A mediates retinoic acid-induced decreases in phosphorylation of endothelial nitric oxide synthase at serine 1179 and nitric oxide production in bovine aortic endothelial cells. *Biochem Biophys Res Commun*. 2013;430(2):476-481.

64. May P, Herz J, Bock HH. Molecular mechanisms of lipoprotein receptor signalling. *Cell Mol Life Sci*. 2005;62(19-20):2325-2338.

65. Herz J, Chen Y. Reelin, lipoprotein receptors and synaptic plasticity. *Nat Rev Neurosci*. 2006;7(11):850-859.

66. Urbanus RT, Pennings MT, Derksen RH, de Groot PG. Platelet activation by dimeric beta2-glycoprotein I requires signaling via both glycoprotein Ibalpha and apolipoprotein E receptor 2′. *J Thromb Haemost*. 2008;6(8):1405-1412.

67. Yang XV, Banerjee Y, Fernández JA, et al. Activated protein C ligation of ApoER2 (LRP8) causes Dab1-dependent signaling in U937 cells. *Proc Natl Acad Sci USA*. 2009;106(1):274-279.

68. Finkielstein CV, Capelluto DG. Disabled-2: A modular scaffold protein with multifaceted functions in signaling. *BioEssays*. 2016;38(suppl 1):S45-S55.

69. Cuitino L, Matute R, Retamal C, Bu G, Inestrosa NC, Marzolo MP. ApoER2 is endocytosed by a clathrin-mediated process involving the adaptor protein Dab2 independent of its Rafts' association. *Traffic*. 2005;6(9):820-838.

70. Tanigaki K, Chambliss KL, Yuhanna IS, et al. Endothelial Fcγ receptor IIB activation blunts insulin delivery to skeletal muscle to cause insulin resistance in mice. *Diabetes*. 2016;65(7):1996-2005.

71. Beffert U, Weeber EJ, Durudas A, et al. Modulation of synaptic plasticity and memory by Reelin involves differential splicing of the lipoprotein receptor Apoer2. *Neuron*. 2005;47(4):567-579.

72. Sangodkar J, Farrington CC, McClinch K, Galsky MD, Kastrinsky DB, Narla G. All roads lead to PP2A: exploiting the therapeutic potential of this phosphatase. *FEBS J*. 2016;283(6):1004-1024.

73. Guergnon J, Dessauge F, Dominguez V, et al. Use of penetrating peptides interacting with PP1/PP2A proteins as a general approach for a drug phosphatase technology. *Mol Pharmacol*. 2006;69(4):1115-1124.

74. McConnell JL, Wadzinski BE. Targeting protein serine/threonine phosphatases for drug development. *Mol Pharmacol*. 2009;75(6):1249-1261.

75. Stanevich V, Jiang L, Satyshur KA, et al. The structural basis for tight control of PP2A methylation and function by LCMT-1. *Mol Cell*. 2011;41(3):331-342.

76. Wu RF, Liao C, Fu G, et al. p66Shc couples mechanical signals to RhoA through FAK-dependent recruitment of p115-RhoGEF and GEF-H1 [published online ahead of print 29 August 2016]. *Mol Cell Biol*. doi:10.1128/MCB.00194-16.

77. Ma Z, Myers DP, Wu RF, Nwariaku FE, Terada LS. p66Shc mediates anoikis through RhoA. *J Cell Biol*. 2007;179(1):23-31.

78. Kim CS, Jung SB, Naqvi A, et al. p53 impairs endothelium-dependent vasomotor function through transcriptional upregulation of p66shc. *Circ Res*. 2008;103(12):1441-1450.

79. Yamamori T, White AR, Mattagajasingh I, et al. P66shc regulates endothelial NO production and endothelium-dependent vasorelaxation: implications for age-associated vascular dysfunction. *J Mol Cell Cardiol*. 2005;39(6):992-995.

80. Urbanus RT, Derksen RH, de Groot PG. Platelets and the antiphospholipid syndrome. *Lupus*. 2008;17(10):888-894.

81. Vega-Ostertag ME, Pierangeli SS. Mechanisms of aPL-mediated thrombosis: effects of aPL on endothelium and platelets. *Curr Rheumatol Rep*. 2007;9(3):190-197.

82. Nabzdyk CS, Pradhan-Nabzdyk L, LoGerfo FW. RNAi therapy to the wall of arteries and veins: anatomical, physiologic, and pharmacological considerations. *J Transl Med*. 2017;15(1):164.

83. Dronadula N, Wacker BK, Van Der Kwast R, Zhang J, Dichek DA. Stable in vivo transgene expression in endothelial cells with helper-dependent adenovirus: roles of promoter and interleukin-10. *Hum Gene Ther*. 2017;28(3):255-270.

84. Dahlman JE, Barnes C, Khan O, et al. In vivo endothelial siRNA delivery using polymeric nanoparticles with low molecular weight. *Nat Nanotechnol*. 2014;9(8):648-655.

85. Fehring V, Schaeper U, Ahrens K, et al. Delivery of therapeutic siRNA to the lung endothelium via novel Lipoplex formulation DACC. *Mol Ther*. 2014;22(4):811-820.

86. Sager HB, Dutta P, Dahlman JE, et al. RNAi targeting multiple cell adhesion molecules reduces immune cell recruitment and vascular inflammation after myocardial infarction. *Sci Transl Med*. 2016;8(342):342ra80.